Int. J. Solids Structures Vol. 24, No. 9, pp. 963–972, 1988
Printed in Great Britain.

0020–7683/88 $3.00+ .00

A NOTE ON THE ELASTODYNAMIC LOAD TRANSFER PROBLEM

R. K. N. D. RAJAPAKSE
Department of Civil Engineering, University of Manitoba, Winnipeg, Canada R3T 2N2

(*Received* 15 *July* 1987; *in revised form* 17 *March* 1988)

Abstract—This paper illustrates the solution of elastodynamic load transfer problems involving a cylindrical elastic bar partially embedded in a homogeneous isotropic elastic half space using a solution scheme based on a coupled variational–boundary integral equation algorithm. The present solution scheme has several advantages over conventional schemes based on the fictitious bar–extended half space model when applied to solve elastodynamic load transfer problems. The analysis ensures limited *displacement compatibility* and *traction continuity* along the *true contact surface* between the bar and the half space. The solution scheme is based on an elastodynamic variational principle and utilizes appropriate Green's function representations for the surrounding half space. Selected numerical results for torsional and axial impedances of the bar–half space system are presented and these are compared with those obtained previously on the basis of the fictitious bar–extended half space model. In addition, the bar displacement and the bar stress resultant profiles are presented for torsion and axial load transfer problems to portray the dependence of the load diffusion on the governing parameters of the bar–half space system.

INTRODUCTION

The time-harmonic response of a long finite cylindrical elastic bar which is partially embedded in a homogeneous isotropic elastic half space has been considered recently (Rajapakse and Shah, 1987a, b; Rajapakse *et al.*, 1987) on the basis of the fictitious bar–extended half space model originally proposed by Muki and Sternberg (1969, 1970) for the elastostatic case. It was noted (Rajapakse and Shah, 1987a) that the elastostatic load transfer solution schemes can be used for elastodynamic problems only for very low frequencies. A modified solution scheme based on a non-uniform body force field acting on the extended half space is presented (Rajapakse and Shah, 1987a, b) to study time-harmonic vibrations of a bar–half space system over a wide range of frequencies. It was also observed (Rajapakse and Shah, 1987a) that the impedance solutions of the bar–half space system show considerable dependence on the location of the compatibility selected for the extended half space.

These observations and the inapplicability of the fictitious bar–extended half space model to non-homogeneous and anisotropic media led to a novel solution scheme which is based on a coupled variational–boundary integral equation formulation (Rajapakse, 1988). The solution scheme (Rajapakse, 1988) is based on a decomposition involving a one-dimensional elastic bar and an elastic half space with a cavity identical to the bar. In view of this *appropriate displacement compatibility* and *traction continuity* can be achieved along the *true contact surface* between the bar and the surrounding elastic medium. The main objective of this paper is to illustrate the application of the coupled variational–boundary integral equation solution scheme to elastodynamic load transfer problems by reconsidering the torsional and axial load transfer problems. The advantages of the present scheme for an elastodynamic problem when compared to a solution based on the fictitious bar–extended half space model are given below.

(a) The compatibility of the major displacement and the continuity of traction are achieved along the true contact surface and this is more realistic than treating fictitious systems.

(b) The fictitious bar–extended half space model provides several options in selecting a suitable compatibility condition between the extended half space and the fictitious bar. In the case of elastodynamic problems it has been found (Rajapakse and Shah, 1987a) that the impedance solutions of the bar–half space system show considerable dependence on the

location of the compatibility selected in the analysis for the extended half space. In contrast, the proposed coupled variational–boundary integral equation scheme is based on a unique and real compatibility condition and results in a unique solution.

(c) The accurate treatment of inertia terms is no longer a problem since the deformation of a real bar is consistent and truly one-dimensional. Since the decomposition does not involve an extended half space, inertia terms are properly quantified and incorporated into the analysis.

(d) The case of an elastic bar with a mass density less than the surrounding half space (e.g. wood piles) can be treated without any ambiguity. It should be mentioned here that when the real bar mass density is less than that of the surrounding half space the use of the fictitious bar–extended half space model results in a fictitious bar with a negative mass density.

(e) Unlike in the case of the fictitious bar–extended half space model, the solution obtained from the present scheme for the limiting case of a rigid bar corresponds to the exact boundary-value problem associated with a rigid bar embedded in an elastic half space.

(f) The computation of the bar displacements and stress resultants becomes consistent, simple and numerically efficient.

CYLINDRICAL ELASTIC BAR EMBEDDED IN A HALF SPACE

Consider the case of a cylindrical elastic bar of radius a (the entire problem is non-dimensionalized by defining "a" as a unit length) and length h ($h/a \gg 1$) partially embedded in an elastic half space. A cylindrical coordinate system (r, θ, z) is used in the analysis with the z-axis identical to the centroidal axis of the cylinder and normal to the stress-free surface of the half space. The Young's modulus and mass density of the bar are denoted by E_b and ρ_b, respectively. The Young's modulus, Poisson's ratio and the mass density of the surrounding half space are denoted by E, ν and ρ, respectively. The motion is time harmonic and the term $e^{i\omega t}$ is suppressed in the sequel.

Following a previous study (Rajapakse, 1988), the bar–half space system is decomposed into an elastic half space $\bar{\mathbf{B}}$ with a cylindrical cavity identical to the bar and the real bar B. In the analysis $\bar{\mathbf{B}}$ and B are treated using three- and one-dimensional continuum theory, respectively. Note that a one-dimensional continuum model can be adopted for B only at low frequencies of excitation. A rigorous solution for torsional dispersion relations is given by Kleczewski and Parnes (1987) for the case of an infinitely long elastic bar bonded to a surrounding elastic full space. These authors (Kelczewski and Parnes, 1987) also compared numerical solutions for roots of the dispersion equation based on the three-dimensional model with those based on a one-dimensional continuum model for the infinitely long bar (Parnes, 1982) to establish the validity of the one-dimensional model for low frequencies.

First consider the case where the bar is subjected to a time-harmonic torque $T_0 e^{i\omega t}$ at $z = 0$. The displacement in the θ-direction of bar B denoted by $u_{\theta b}$ can be expressed in the admissible form

$$u_{\theta b}(r, z, t) = \sum_{n=1}^{N} \alpha_n(t) r \, e^{-(n-1)z/h} \tag{1}$$

$$\dot{u}_{\theta b}(r, z, t) = \sum_{n=1}^{N} \dot{\alpha}_n(t) r \, e^{-(n-1)z/h} \tag{2}$$

where $\alpha_1, \ldots, \alpha_n$ can be viewed as generalized coordinates and the superscript dot denotes differentiation with respect to time.

Since the compatibility exists between B and $\bar{\mathbf{B}}$ the displacement in the θ-direction on the cylindrical cavity surface S of $\bar{\mathbf{B}}$ is given by eqn (1). For an axisymmetric pure torsion problem the only non-trivial displacement is in the θ-direction and on surface S only the traction in the θ-direction is nonzero. The application of integral representation theorems (Eringen and Suhubi, 1975) to $\bar{\mathbf{B}}$ with respect to a set of nodal points on S leads to

$$\{T_\theta\} = [K]_\theta \{\bar{u}_\theta\} \tag{3}$$

where $\{\bar{u}_\theta\}$ and $\{T_\theta\}$ denote column vectors, the elements of which are displacements and tractions in the θ-direction at nodal locations on S. An explicit representation for $[K]_\theta$ is yet to be determined.

Noting that

$$\bar{u}_\theta = \sum_{n=1}^{N} \alpha_n \bar{u}_{\theta n} \tag{4a}$$

where

$$\bar{u}_{\theta n} = r\, \mathrm{e}^{-(n-1)z/h}, \quad (r, z) \in \mathrm{S} \tag{4b}$$

the traction T_θ on S may be expressed as

$$T_\theta = \sum_{n=1}^{N} \alpha_n T_{\theta n} \tag{5}$$

where $T_{\theta n}$ denotes the traction on S of $\bar{\mathrm{B}}$ corresponding to $\bar{u}_{\theta n}$ given by eqn (4b).

In view of eqn (3)

$$\{T_{\theta n}\} = [K]_\theta \{\bar{u}_{\theta n}\}. \tag{6}$$

The Lagrangian L of the bar B can be expressed as (Washishu, 1982)

$$L = L_{\mathrm{b}} - \frac{1}{2}\int_{\mathrm{S}} \bar{u}_\theta T_\theta \, \mathrm{dS} + T_0 \sum_{n=1}^{N} \alpha_n. \tag{7}$$

In eqn (7), L_{b} denotes the Lagrangian function (Washishu, 1982) of bar B and the term involving the surface integral over S denotes the contribution due to traction T_θ acting on S.

In view of eqn (1), L_{b} can be expressed as

$$L_{\mathrm{b}} = \sum_{n=1}^{N} \sum_{m=1}^{N} [\dot{\alpha}_n \dot{\alpha}_m C_{mn} - \alpha_n \alpha_m D_{mn}] \tag{8}$$

where

$$C_{mn} = \pi \rho_{\mathrm{b}} a^4 h (1 - \mathrm{e}^{-(m+n-2)})/[4(m+n-2)], \quad m+n \neq 2 \tag{9}$$

$$D_{mn} = \pi \mu_{\mathrm{b}} a^4 (n-1)(m-1)(1 - \mathrm{e}^{-(m+n-2)})/[4h(n+m-2)], \quad m+n \neq 2 \tag{10}$$

and

$$C_{11} = \frac{\pi \rho_{\mathrm{b}} a^4 h}{4}; \quad D_{11} = 0. \tag{11}$$

The substitution of eqns (3)–(6) and (8) in eqn (7) yields an expression for L which is indeterminate with respect to the generalized coordinates α_n and $\dot{\alpha}_n$ ($n = 1, \ldots, N$). These generalized coordinates are determined through the application of Lagrange's equation of motion (Washishu, 1982) and this together with the fact that the motion is time harmonic leads to the following equations of motion of B:

$$\sum_{n=1}^{N} \alpha_n \left[-2\omega^2 C_{ni} + 2D_{ni} + \sum_{j=1}^{M} (T_{\theta nj}\bar{u}_{\theta ij} + T_{\theta ij}\bar{u}_{\theta nj}) A_j/2 \right] = T_0 \quad (i = 1, 2, \ldots, N) \tag{12}$$

where

$$T_{\theta nj} = T_{\theta n}(r_j, z_j), \quad (r_j, z_j) \in \mathrm{S}, j = 1, \ldots, M \tag{13a}$$

$$\bar{u}_{\theta nj} = u_{\theta n}(r_j, z_j), \quad (r_j, z_j) \in \mathrm{S}, j = 1, \ldots, M \tag{13b}$$

$$A_j = \text{tributary area of node } j \text{ on S} \tag{13c}$$

and M is the total number of nodes used to discretize S.

The numerical solution of eqn (12) results in values for α_i $(i = 1, \ldots, N)$. The resultant torque $T_b(z)$ acting on the bar cross-section at a depth z is given by

$$T_b(z) = \mu_b J \sum_{n=1}^{N} \alpha_n u'_{\theta b}(a, z) \tag{14}$$

where

$$u'_{\theta b}(a, z) = \frac{\mathrm{d}u_{\theta b}(a, z)}{\mathrm{d}z} \tag{15}$$

and

$$J = \pi a^4/2. \tag{16}$$

Next, consider the case where the bar–half space system is subjected to an axial load $P_0 \, \mathrm{e}^{\mathrm{i}\omega t}$ at the top end of the bar. The bar displacement in the z-direction denoted by u_{zb} can be represented in the following admissible one-dimensional form:

$$u_{zb}(z, t) = \sum_{n=1}^{N} \alpha_n(t)(z/h)^{n-1}. \tag{17}$$

Due to the different order of the continuum models employed for B and $\bar{\mathrm{B}}$ exact displacement compatibility along contact surface S cannot be achieved. It is proposed to impose displacement compatibility only in the z-direction between B and $\bar{\mathrm{B}}$ on contact surface S. Therefore, the displacement in the z-direction at locations on S of $\bar{\mathrm{B}}$ is given by eqn (17). In order to define a unique boundary-value problem for $\bar{\mathrm{B}}$ to determine traction T_z on S due to the displacement field given by eqn (17) it is also necessary to define a proper boundary condition on S in the r-direction, either in terms of displacement or traction. Noting that for the case of a rigid bar $(E_b \to \infty)$ $u_r \equiv 0$ on S, it is proposed to impose this boundary condition on S. The other alternative is to take traction $T_r \equiv 0$ on S but this cannot be related to a realistic limiting case. Note that in this axisymmetric problem $u_\theta \equiv 0$ in $\bar{\mathrm{B}}$.

Consider the boundary-value problem for $\bar{B}$ with the following displacement boundary conditions on S:

$$\bar{u}_{zn}(r, z) = (z/h)^{n-1}, \quad (r, z) \in \mathrm{S} \tag{18a}$$

$$\bar{u}_{rn}(r, z) = 0, \qquad (r, z) \in \mathrm{S}. \tag{18b}$$

Let $T_{zn}(r, z)$ and $T_{rn}(r, z)$ denote tractions in the z- and r-directions on S corresponding to the displacement field given by eqns (18). Using representation theorems (Eringen and Suhubi, 1975) and a set of nodal points on S, the following relationship similar to eqn (3) can be established:

$$\begin{Bmatrix} \{T_{zn}\} \\ \{T_{rn}\} \end{Bmatrix} = [K]_z \begin{Bmatrix} \{\bar{u}_{zn}\} \\ \{\bar{u}_{rn}\} \end{Bmatrix}. \tag{19}$$

In view of eqn (18b)

$$\{\bar{u}_{rn}\} = \{0\}. \tag{20}$$

The Lagrangian L for the axial loading problem is given by

$$L = L_b - \frac{1}{2}\int_S (\bar{u}_z T_z + \bar{u}_r T_r)\, dS + P_0\alpha_1 \tag{21a}$$

where

$$T_z = \sum_{n=1}^{N} \alpha_n T_{zn}; \quad T_r = \sum_{n=1}^{N} \alpha_n T_{rn} \tag{21b}$$

and

$$\bar{u}_z = \sum_{n=1}^{N} \alpha_n \bar{u}_{zn}; \quad \bar{u}_r = \sum_{n=1}^{N} \alpha_n \bar{u}_{rn}. \tag{21c}$$

Note that in view of eqn (18b) the second term of the surface integral in eqn (21a) vanishes and L_b in eqn (21a) is given by eqn (8) with C_{mn} and D_{mn} defined as

$$C_{mn} = \frac{\pi a^2 \rho_b h}{2(n+m-1)} \tag{22a}$$

$$D_{mn} = \frac{\pi a^2 E_b (n-1)(m-1)}{2h(n+m-3)}, \quad n+m \neq 3 \tag{22b}$$

$$= 0, \qquad n+m = 3.$$

The substitution of eqns (8), (17)–(20), (21b) and (21c) in eqn (21a) results in an expression for the Lagrangian function L in terms of α_n and $\dot{\alpha}_n$ ($n = 1, \ldots, N$). Thereafter the application of Lagrange's equation of motion (Washishu, 1982) results in the following equations of motion to determine α_n ($n = 1, \ldots, N$):

$$\sum_{n=1}^{N} \alpha_n \left[-2\omega^2 C_{ni} + 2D_{ni} + \sum_{j=1}^{M} [T_{znj}\bar{u}_{zij} + T_{zij}\bar{u}_{znj}] A_j/2 \right] = P_0 \delta_{1i} \quad (i = 1, \ldots, N) \tag{23}$$

where

$$T_{znj} = T_{zn}(r_j, z_j), \quad (r_j, z_j) \in S, j = 1, \ldots, M \tag{24a}$$

$$\bar{u}_{znj} = u_{zn}(r_j, z_j), \quad (r_j, z_j) \in S, j = 1, \ldots, M \tag{24b}$$

$$\delta_{ik} = \text{Kronecker's delta function.} \tag{24c}$$

The resultant axial force $P_b(z)$ acting on a bar cross-section at a depth z is given by

$$P_b(z) = E_b \pi a^2 \sum_{n=1}^{N} \alpha_n (n-1)(z/h)^{n-2}/h. \tag{25}$$

EXPLICIT REPRESENTATIONS FOR $[K]_\theta$ AND $[K]_z$

The derivation of the explicit representations for $[K]_\theta$ and $[K]_z$ that are necessary to compute vectors $\{T_{\theta n}\}$ and $\{T_{zn}\}$, the elements of which appear in eqns (12) and (23), is discussed in this section. The previous study (Rajapakse, 1988) demonstrates the application

of the indirect boundary integral equation method proposed by Ohsaki (1973) to determine the traction–displacement relationship along the surface of a cylindrical cavity created in an elastic half space. In this method a uniform half space B* without a cavity is considered. A surface S′ representing the true contact surface is also defined in B*. Interior to S′, an arbitrary surface S* with geometry similar to S′ is defined. Surfaces S′ and S* are discretized into M and M^* ring elements with one element of circular disc shape representing the base level. A body force field τ_i^* ($i = \theta$ for the torsion problem; $i = r, z$ for the axial load problem), is applied on S* such that the displacement in the i-direction on S′ is equal to that given by eqns (4b) and (18) for torsion and axial load transfer problems, respectively. It can be shown that (Ohsaki, 1973; Rajapakse, 1988)

$$[K]_m = [\bar{H}^{pq}][[\bar{G}^{pq}]^{\mathrm{T}}[\bar{G}^{pq}]]^{-1}[\bar{G}^{pq}]^{\mathrm{T}} \tag{26a}$$

where

$$m = p = q = \theta \tag{26b}$$

for the torsion load transfer problem, and

$$m = z \text{ and } p, q = r, z \tag{26c}$$

for the axial load transfer problem.

The elements $\bar{H}_{ij}^{pq}$ and $\bar{G}_{ij}^{pq}$ of $[\bar{H}^{pq}]$ and $[\bar{G}^{pq}]$ are defined as

$$\bar{H}_{ij}^{pq} = H_{pq}(r_i, z_i; r_j^*, z_j^*)\, \mathrm{dS}_j^* \tag{27a}$$

$$\bar{G}_{ij}^{pq} = G_{pq}(r_i, z_i; r_j^*, z_j^*)\, \mathrm{dS}_j^* \tag{27b}$$

In eqns (27), $H_{pq}(r_i, z_i; r_j^*, z_j^*)$ and $G_{pq}(r_i, z_i; r_j^*, z_j^*)$ denote traction (on a plane with unit normal $\mathbf{n}$) and displacement in the p-direction, respectively, at point $(r_i, z_i) \in \mathrm{S}'$ due to a time-harmonic ring load in the q-direction through point $(r_j^*, z_j^*) \in \mathrm{S}^*$; dS_j^* denotes the tributary area of ring element j on S*. Note that $G_{pq}(r_i, z_i; r_j^*, z_j^*)$ corresponding to torsion and axial load transfer problems have been previously presented explicitly (Rajapakse *et al.*, 1987; Rajapakse and Shah, 1987a). Explicit representations for $H_{pq}(r_i, z_i; r_j^*, z_j^*)$ can be derived from $G_{pq}(r_i, z_i; r_j^*, z_j^*)$ using basic relationships in elasticity. The order of $[\bar{H}^{pq}]$ and $[\bar{G}^{pq}]$ for the torsion problem is $M \times M^*$ and $2M \times 2M^*$ for the axial load transfer problem. In view of eqn (19), for the axial load transfer problem $[H^{pq}]$ is set up in the following format:

$$[\bar{H}^{pq}] = \begin{bmatrix} [\bar{H}_{ij}^{zz}] & [\bar{H}_{ij}^{zr}] \\ [\bar{H}_{ij}^{rz}] & [\bar{H}_{ij}^{rr}] \end{bmatrix} \tag{28}$$

and $[\bar{G}^{pq}]$ also has a similar format.

DISCUSSION AND CONCLUSIONS

A numerical study was performed by varying the number of nodal locations (M and M^*) on S′ and S* and the number of terms (N) used in the displacement approximations given by eqns (1) and (17) to determine the numerical stability and convergence of the present solution scheme. It was found that for $0 \leqslant a_0 \leqslant 1.5$ (where $a_0 = ak_s$ and k_s is the shear wave number of the surrounding half space) solutions converge for $N = 8$ for most bar lengths. For the case of a bar with $h/a = 10.0$ and $0 \leqslant a_0 \leqslant 1.5$ solutions converge when $M = 40$ and $M^* = 25$. It should be mentioned here that the use of a very large value for N and an extremely fine discretization on S′ and S* may lead to numerical instability. Details of the convergence and stability study are not presented here for brevity.

It is important to mention here that the main numerical effort in the solution scheme is associated with the establishment of $[K]_\theta$ and $[K]_z$ given by eqn (26a). The evaluation of $[\bar{H}^{pq}]$ and $[\bar{G}^{pq}]$ involves the numerical integration of complex-valued infinite integrals

involving products of Bessel functions. Proper attention should be paid to the singularities and the oscillating nature of the integrand in the numerical integration scheme.

Table 1 presents a comparison of solutions for non-dimensionalized torsional impedance, K_T ($K_T = 3T_0/16\mu a^3\phi_0$, where ϕ_0 is the rotation of the bar at the top end) obtained from the present scheme and those reported previously (Rajapakse *et al.*, 1987) based on the fictitious bar–extended half space model. The agreement between solutions obtained from the two different schemes is very close. It should be mentioned here that by virtue of the model considered (Rajapakse *et al.*, 1987), the displacement in the domain of the extended half space corresponding to the bar is not totally compatible with the one-dimensional deformation of the fictitious bar. Therefore, with increasing a_0 inertia terms cannot be properly accounted for and consequently the solution is distorted. The author has studied displacement profiles of the extended half space and found that within the range $0 \leqslant a_0 \leqslant 1.5$ the use of the fictitious bar–extended half space model yields results with reasonable accuracy for the torsion problem. This fact is also confirmed by the numerical results presented in Table 1.

Table 2 presents a comparison of solutions for axial impedance, K_v ($K_v = P_0/\mu a\Delta_0$, where Δ_0 is the vertical displacement at the top end of the bar) obtained from the present scheme with those of a previous study (Rajapakse and Shah, 1987a) by using the fictitious bar–extended half space model with a non-uniform body force applied on the extended half space. Solutions presented in Table 2 agree very closely confirming the accuracy of the solution scheme proposed (Rajapakse and Shah, 1987a). Differences in numerical solutions noted in Table 2 with increasing a_0 can be attributed to the fact that in the solution scheme proposed previously (Rajapakse and Shah, 1987b) the compatibility between the fictitious bar and the extended half space is imposed discretely within the domain of the extended half space corresponding to the bar.

The comparison of numerical solutions for K_v presented in Table 2 with those presented previously (Table 5 of the study by Rajapakse and Shah (1987a)) confirms the *inaccuracy* of the elastodynamic solutions based on a uniform body force model with the *displacement compatibility imposed along the z-axis of the extended half space.* Further comparisons of K_v solutions (Rajapakse and Shah, 1987a) with those obtained in the present study indicate that reasonably accurate solutions can be obtained by using the uniform body force model provided the compatibility is imposed along the fictitious contact surface ($r = a$, $0 \leqslant z \leqslant h$) in the extended half space and the non-dimensionalized frequency of excitation is less than 0.5.

In the present solution scheme the bar displacement and stress resultant profiles can be computed simply using eqns (1), (14), (17) and (25) when compared to more involved

Table 1. Comparison of non-dimensionalized torsional impedance (K_T) for an elastic bar; $h/a = 10.0$, $\bar{\rho} = 1.0$, $M = 40$, $M^* = 25$, $N = 8$, $r^* = 0.9$

	$K_T = 3T_0/16\mu a^3\phi_0$			
	$\bar{\mu} = 10$		$\bar{\mu} = 100$	
a_0	Rajapakse *et al.* (1987)	Present study	Rajapakse *et al.* (1987)	Present study
0.50	(2.61, 0.11)	(2.70, 0.11)	(7.89, 0.59)	(7.98, 0.57)
1.00	(2.41, 0.48)	(2.45, 0.49)	(7.30, 1.90)	(7.40, 1.92)
1.50	(2.26, 0.95)	(2.28, 0.97)	(6.92, 3.47)	(7.06, 3.45)

Table 2. Comparison of non-dimensionalized vertical impedance (K_v) for an elastic bar; $h/a = 10.0$, $\bar{\rho} = 1.0$, $\nu = 0.25$, $M = 40$, $M^* = 25$, $N = 8$, $r^* = 0.9$

	$K_v = P_0/\mu a\Delta_0$					
	$a_0 = 0.4$		$a_0 = 1.0$		$a_0 = 1.5$	
$\bar{E}$	Rajapakse and Shah (1987a)	Present study	Rajapakse and Shah (1987a)	Present study	Rajapakse and Shah (1987a)	Present study
10	(14.35, 8.40)	(14.36, 8.29)	(16.04, 16.62)	(15.56, 16.20)	(15.01, 24.06)	(13.89, 23.53)
50	(23.16, 21.31)	(23.20, 20.89)	(25.82, 49.14)	(26.36, 49.26)	(35.39, 74.21)	(37.82, 73.77)
100	(24.06, 25.00)	(24.68, 26.04)	(17.92, 61.90)	(18.64, 63.46)	(13.04, 104.4)	(14.42, 107.8)
1000	(24.31, 32.81)	(25.24, 32.81)	(2.61, 71.31)	(1.94, 72.96)	(−34.91, 107.2)	(−37.34, 109.7)

procedures required for solutions based on the fictitious bar–extended half space model (Muki and Sternberg, 1970; Karasudhi *et al.*, 1984). Figure 1 shows the variation of the non-dimensionalized bar twist angle $\bar{\phi}(z)$ [$\bar{\phi}(z) = \mu a^2 u_{0b}(z)/T_0$] and the bar torque $\bar{T}_b(z)$ [$\bar{T}_b(z) = T_b(z)/T_0$] along the bar length with bar flexibility ratio $\bar{\mu}$ ($\bar{\mu} = \mu_b/\mu$), non-dimensionalized frequency a_0 and mass density ratio $\bar{\rho}$ ($\bar{\rho} = \rho_b/\rho$). It is noted that the real part of $\bar{\phi}(z)$ shows considerable dependence on $\bar{\mu}$ but the imaginary component is less affected by $\bar{\mu}$. Solutions for bar torque profiles indicate that both the real and imaginary parts of $\bar{T}_b(z)$ have considerable dependence on $\bar{\mu}$. Solutions presented in Fig. 1(b) indicate that the real and imaginary components of $\phi(z)$ and the imaginary component of $\bar{T}_b(z)$ depend significantly on a_0. However, the real part of $\bar{T}_b(\bar{z})$ is found to have a negligible variation with a_0. The dependence of solutions on $\bar{\rho}$ is found to be similar to that for a_0. It is noted that if the bar is quite flexible (low $\bar{\mu}$) and a_0 is smaller ($a_0 < 1.0$), then $\bar{\rho}$ has a negligible influence on solutions.

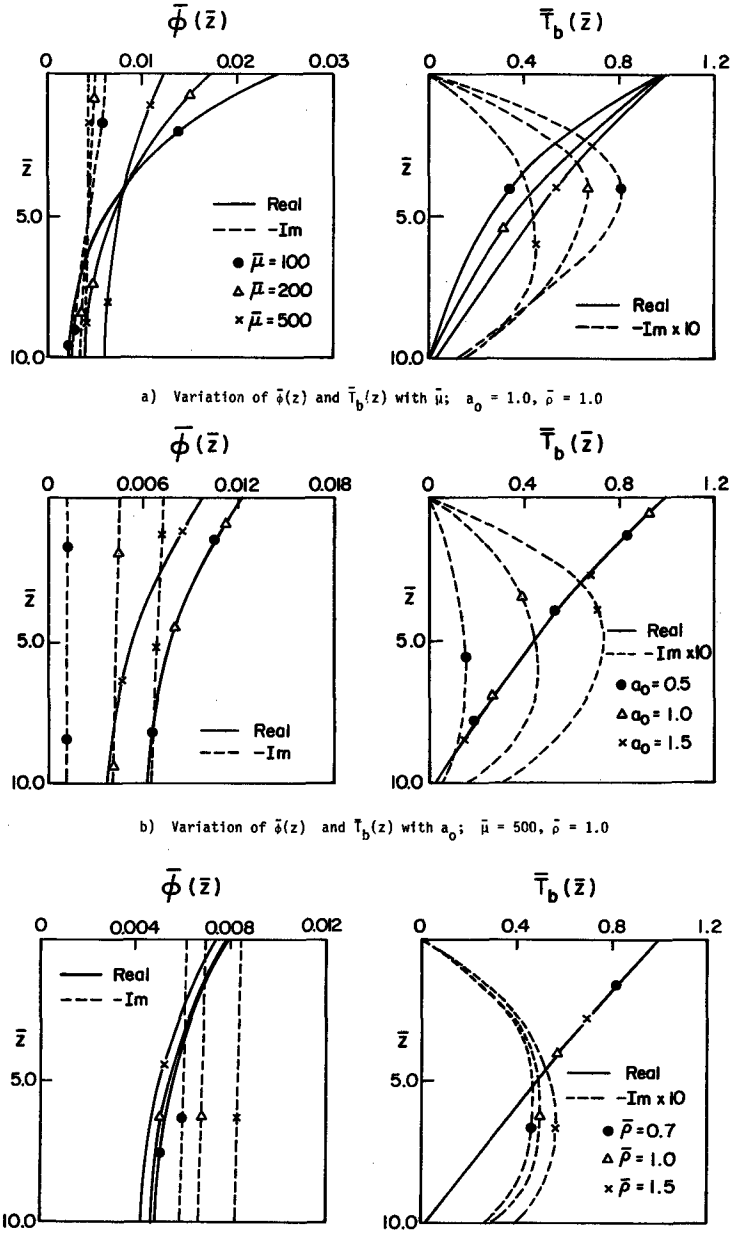

Fig. 1. Bar rotation [$\bar{\phi}(z)$] and torque [$\bar{T}_b(z)$] profiles for torsion load transfer problem; $h/a = 10.0$, $N = 8$, $M = 40$, $M^* = 25$, $r^* = 0.9$.

Figures 2(a)–(c) show the variation of the non-dimensionalized vertical displacement $\bar{u}_{zb}(z)$ [$\bar{u}_{zb}(z) = \mu a u_{zb}(z)/P_0$] and the axial force $\bar{P}_b(z)$ [$\bar{P}_b(z) = P_b(z)/P_0$] along the bar length with the bar flexibility ratio $\bar{E}$ ($\bar{E} = E_b/E$), non-dimensionalized frequency a_0, and mass density ratio $\bar{\rho}$. It is noted from Fig. 2(a) that both $\bar{u}_{zb}$ and $\bar{P}_b(z)$ have a significant dependence on $\bar{E}$ and the most interesting feature is the reversal of the sign of the displacement profile. A similar behaviour is noted in the bar force profile for very flexible bars. Figure 2(b) indicates that with increasing a_0 bar displacement profiles change sign and such a reversal of sign is also noted in bar force profiles near the base of the bar. Figure 2(c) shows that an increase in the bar mass density results in a decrease in the real part of $\bar{u}_{zb}$ and has a negligible influence on the imaginary part of $\bar{u}_{zb}$ and bar force profiles. As $\bar{\rho}$ increases the location on the bar where the real part of $\bar{u}_{zb}$ is zero moves upward making the change in sign of Re ($\bar{u}_{zb}$) more prominent.

An alternative formulation to the elastodynamic load transfer problem could be obtained by coupling the traction–displacement relationships given by eqns (3) and (19)

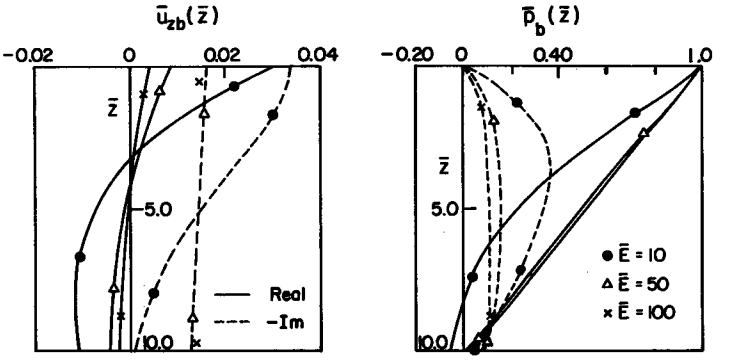

a) Variation of $\bar{u}_{zb}(z)$ and $\bar{P}_b(z)$ with $\bar{E}$; $a_0 = 1.0$, $\bar{\rho} = 1.0$

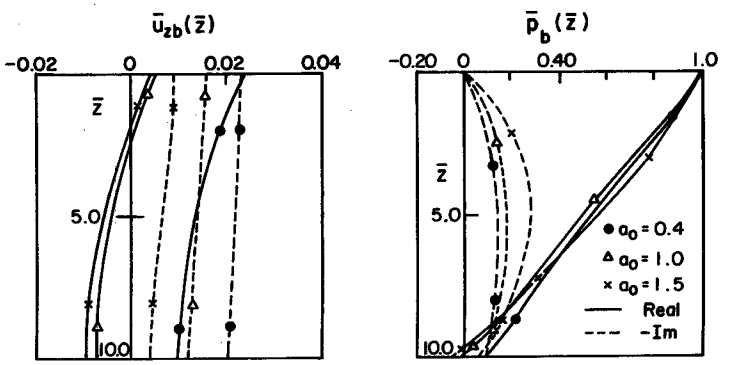

b) Variation of $\bar{u}_{zb}(z)$ and $\bar{P}_b(z)$ with a_0, $\bar{E} = 50$, $\bar{\rho} = 1.5$

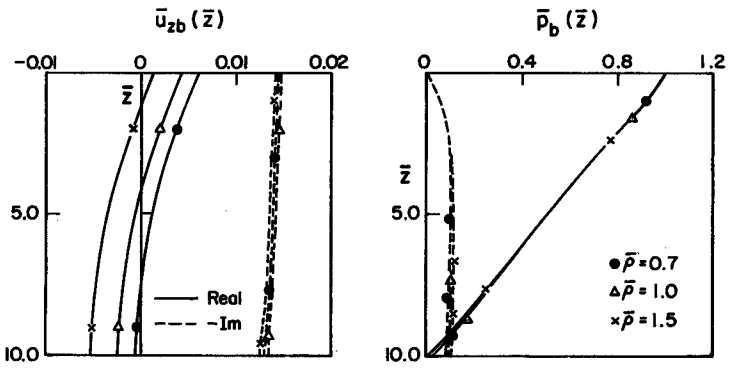

c) Variation of $\bar{u}_{zb}(z)$ and $\bar{P}_b(z)$ with $\bar{\rho}$; $\bar{E} = 100$, $a_0 = 1.0$

Fig. 2. Axial displacement [$\bar{u}_{zb}(z)$] and axial force [$\bar{P}_b(z)$] profiles of bar for axial load transfer problem; $h/a = 10.0$, $\nu = 0.25$, $N = 8$, $M = 40$, $M^* = 25$, $r^* = 0.9$.

with a finite-difference version of an appropriate one-dimensional governing equation of the bar. The finite-difference representation incorporated with relevant boundary conditions results in a linear simultaneous equation for displacement at the nodal locations along the bar length. However, in the author's opinion the coupled variational–boundary integral equation solution scheme is more accurate than a coupled finite difference–boundary integral equation scheme since the bar displacement field is represented by a set of smooth and continuous basis functions in the variational analysis. The use of a finite difference scheme to represent the bar deformations requires the approximation of displacement derivatives at every nodal point. In addition, bar stress resultant profiles are also computed using additional finite-difference approximations and the resulting solutions may be less accurate.

As concluding remarks one states here that the elastodynamic axial and torsion load transfer problems have been reconsidered on the basis of the solution algorithm proposed previously (Rajapakse, 1988). The present scheme has several advantages over the conventional fictitious bar–extended half space model and these are highlighted in the text. The comparison of solutions for axial impedance confirms the *inaccuracy of solutions based on the fictitious bar–extended half space model with the displacement compatibility on the extended half space imposed along the z-axis.* The coupled variational–boundary integral equation scheme presented in this study provides a consistent and accurate solution for axisymmetric elastodynamic load transfer problems over a wide range of frequency of excitation. The numerical solutions presented in the present study clearly demonstrate the significance of the bar flexibility, frequency of excitation and mass density on the load diffusion and impedance of the bar–half space system. In addition these numerical solutions could provide the basis in determining the accuracy of the finite element and other approximate numerical solutions.

Acknowledgement—The work presented in this paper was supported by Natural Sciences and Engineering Research Council of Canada Grant A-6507.

REFERENCES

Eringen, A. C. and Suhubi, E. H. (1975). *Elastodynamics*, Vol. 2. Academic Press, New York.

Karasudhi, P., Rajapakse, R. K. N. D. and Hwang, B. Y. (1984). Torsion of a long cylindrical elastic bar partially embedded in a layered elastic half space. *Int. J. Solids Structures* **20,** 1–11.

Kleczewski, D. and Parnes, R. (1987). Torsional dispersion relations in a radially dual elastic medium. *J. Acoust. Soc. Am.* **81,** 23–36.

Muki, R. and Sternberg, E. (1969). On the diffusion of axial load from an infinite cylindrical bar embedded in an elastic medium. *Int. J. Solids Structures* **5,** 587–605.

Muki, R. and Sternberg, E. (1970). Elastostatic load transfer to a half-space from a partially embedded axially loaded rod. *Int. J. Solids Structures* **6,** 69–90.

Ohsaki, Y. (1973). On movements of a rigid body in semi-infinite elastic medium. *Proc. Japan Earthq. Engng Symp.*, Tokyo, Japan, pp. 245–252.

Parnes, R. (1982). Torsional dispersion relations of a long infinitely clad cylindrical rod. *J. Acoust. Soc. Am.* **71,** 1347–1351.

Rajapakse, R. K. N. D. (1988). A torsion load transfer problem for a class of non-homogeneous elastic solids. *Int. J. Solids Structures* **24,** 139–151.

Rajapakse, R. K. N. D. and Shah, A. H. (1987a). On the longitudinal harmonic motion of a cylindrical elastic bar embedded in an elastic half space. *Int. J. Solids Structures* **23,** 267–285.

Rajapakse, R. K. N. D. and Shah, A. H. (1987b). On the lateral harmonic motion of a cylindrical elastic bar embedded in an elastic half space. *Int. J. Solids Structures* **23,** 287–303.

Rajapakse, R. K. N. D., Shah, A. H. and Datta, S. K. (1987). Torsional vibrations of elastic foundations embedded in an elastic half space. *Earth Engng Struct. Dyn.* **15,** 279–297.

Washishu, K. (1982). *Variational Methods in Elasticity and Plasticity*, 3rd Edn. Pergamon Press, New York.